European Journal of Pharmaceutical Sciences 120 (2018) 172–180

Contents lists available at ScienceDirect

European Journal of Pharmaceutical Sciences

journal homepage: www.elsevier.com/locate/ejps

N-demethylation of *N*-methyl-4-aminoantipyrine, the main metabolite of metamizole

Fabio Bachmann[a,b], Urs Duthaler[a,b], Deborah Rudin[a,b], Stephan Krähenbühl[a,b,*], Manuel Haschke[c]

[a] Division of Clinical Pharmacology & Toxicology, University Hospital Basel, Switzerland
[b] Department of Biomedicine, University of Basel, Switzerland
[c] Clinical Pharmacology and Toxicology, Department of General Internal Medicine, Inselspital, Bern University Hospital, University of Bern and Institute of Pharmacology, University of Bern, Switzerland

ARTICLE INFO

Keywords:
Metamizole
N-methyl-4-aminoantipyrine
N-demethylation
Cytochrome P450 (CYP)
Myeloperoxidase

ABSTRACT

Metamizole is an old analgesic used frequently in some countries. Active metabolites of metamizole are the non-enzymatically generated *N*-methyl-4-aminoantipyrine (4-MAA) and its demethylation product 4-aminoantipyrine (4-AA). Previous studies suggested that 4-MAA demethylation can be performed by hepatic cytochrome P450 (CYP) 3A4, but the possible contribution of other CYPs remains unclear. Using human liver microsomes (HLM), liver homogenate and HepaRG cells, we could confirm 4-MAA demethylation by CYPs. Based on CYP induction (HepaRG cells) and CYP inhibition (HLM) we could identify CYP2B6, 2C8, 2C9 and 3A4 as major contributors to 4-MAA demethylation. The 4-MAA demethylation rate by HLM was 280 pmol/mg protein/h, too low to account for *in vivo* 4-MAA demethylation in humans. Since peroxidases can perform *N*-demethylation, we investigated horseradish peroxidase and human myeloperoxidase (MPO). Horse radish peroxidase efficiently demethylated 4-MAA, depending on the hydrogen peroxide concentration. This was also true for MPO; this reaction was saturable with a K_m of 22.5 μM and a maximal velocity of 14 nmol/min/mg protein. Calculation of the entire body MPO capacity revealed that the demethylation capacity by granulocyte/granulocyte precursors was approximately 600 times higher than the liver capacity and could account for 4-MAA demethylation in humans. 4-MAA demethylation could also be demonstrated in MPO-expressing granulocyte precursor cells (HL-60). In conclusion, 4-MAA can be demethylated in the liver by several CYPs, but hepatic metabolism cannot fully explain 4-MAA demethylation in humans. The current study suggests that the major part of 4-MAA is demethylated by circulating granulocytes and granulocyte precursors in bone marrow.

1. Introduction

Metamizole (dipyrone) is an analgesic, antipyretic and spasmolytic drug that was introduced in Germany almost 100 years ago. Its mode of action has been investigated in numerous studies but is still not completely elucidated. One study has shown that the two major metabolites of metamizole, *N*-methyl-4-aminoantipyrine (4-MAA) and aminoantipyrine (4-AA) inhibit COX-1 and COX-2 by interfering with Fe^{3+} contained in the heme of the cyclooxygenases (Pierre et al., 2007). However, while the analgesic effect of metamizole is similar to indomethacin, its anti-inflammatory effect is weaker (Tatsuo et al., 1994), suggesting also COX-independent pathways. Multiple additional modes of action have been proposed, among them interaction with the adrenergic nervous system (Silva et al., 2015), modulation of potassium channels (Alves and Duarte, 2002; Duarte et al., 1992; Ortiz et al., 2003), stimulation of the endogenous opioid system (Tortorici et al., 1996; Vanegas et al., 1997; Vasquez and Vanegas, 2000), and interaction with glutamate transmission (Beirith et al., 1998; Siebel et al., 2004) or with the endocannabinoid system (Escobar et al., 2012; Maione et al., 2015). The spasmolytic effect of metamizole is experimentally established, but the mechanism is also not fully clarified. Opening of ATP sensitive potassium channels (Valenzuela et al., 2005) and inhibition of G protein-coupled receptor (GPCR) mediated constriction (Gulmez et al., 2006) of vascular smooth muscle cells are mechanisms currently discussed.

Metamizole is a prodrug that is spontaneously converted to 4-MAA, which has a high oral bioavailability (> 80%) (Ergün et al., 2004). As shown in Figs. 1, 4-MAA can be demethylated to 4-AA or formylated to N-formyl-4-aminoantipyrine (4-FAA). 4-AA can be acetylated to *N*-acetyl-4-aminoantipyrine (4-AAA), which is excreted mainly in the

* Corresponding author at: Clinical Pharmacology & Toxicology, University Hospital, 4031 Basel, Switzerland.
E-mail address: stephan.kraehenbuehl@usb.ch (S. Krähenbühl).

https://doi.org/10.1016/j.ejps.2018.05.003
Received 21 January 2018; Received in revised form 17 April 2018; Accepted 6 May 2018
Available online 08 May 2018
0928-0987/

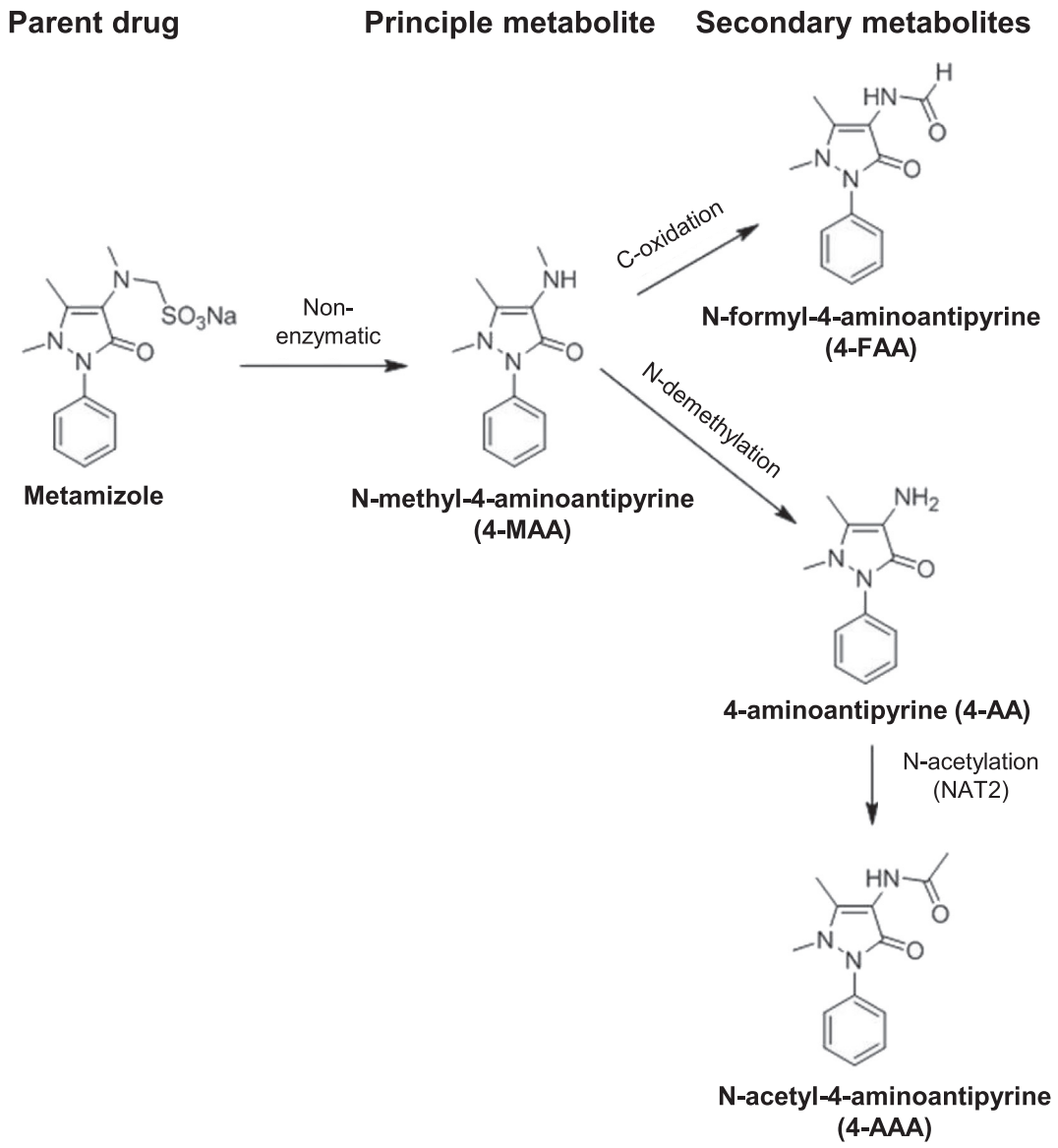

Fig. 1. Metabolism of metamizole. Metamizole is a prodrug efficiently converted non-enzymatically in the intestinal tract to *N*-methyl-4-aminoantipyrine (4-MAA). 4-MAA has a good oral bioavailability (> 80%) and can be converted by C-oxidation to *N*-formyl-4-aminoantiyprine (4-FAA) or by *N*-demethylation to 4-aminoantipyrine (4-AA). 4-AA can be *N*-acetylated by NAT2 to *N*-acetyl-4-aminoantipyrine (4-AAA).

urine. Only 3% of the administered metamizole is excreted in the urine as 4-MAA, the rest is excreted mainly as 4-AA, 4-AAA and 4-FAA as well as additional minor metabolites (Flusser et al., 1988; Levy Micha and Bernd, 1995; Noda et al., 1976a; Noda et al., 1976b; Volz and Kellner, 1980; Zylber-Katz et al., 1992).

Although the four main metabolites of metamizole have been well-described, only the enzyme responsible for the formation of 4-AAA, a polymorphous *N*-acetyltransferase (Agundez et al., 1995; Levy et al., 1984), later identified as *N*-acetyltransferase type 2 (NAT2) (Agundez et al., 1995), has been identified. In contrast, the enzymes involved in the demethylation and formylation of 4-MAA are so far not known. Metabolic studies with the structurally closely related *N*,*N*-dimethyl-4-aminoantipyrine (4-DMAA) have shown that it can be converted at a slow rate to 4-AA in rat liver microsomes (Bast and Noordhoek, 1981; Imaoka et al., 1988; Inoue et al., 1983). Later experiments revealed that approximately 1–2% of 4-MAA could be converted to 4-AA by human liver microsomes (Geisslinger et al., 1996). This process could be partially inhibited by 10 µM ketoconazole (Geisslinger et al., 1996), implicating involvement of CYP 3A4 (Eagling et al., 1998). In humans with impaired liver function, the half-life of 4-MAA is prolonged, supporting the concept that 4-MAA is metabolized by the liver (Agundez et al., 1995; Levy Micha and Bernd, 1995).

Although in most studies concerning *N*-demethylation of 4-DMAA and 4-MAA the involvement of hepatic CYPs was investigated, it has to be taken into account that also other enzymes can perform *N*-demethylation of xenobiotics (Benedetti, 2001; Benedetti et al., 2009). *N*-demethylation of 4-DMAA has for instance been shown for horseradish peroxidase (HRP) (Stiborova et al., 1997) and for soybean lipoxygenase (Perez-Gilabert et al., 1997; Yang and Kulkarni, 1998).

Considering the uncertainties regarding *N*-demethylation of 4-MAA, the aim of the current study was to investigate this step in the metabolism of metamizole in more detail. Therefore, we studied the metabolism of 4-MAA using different hepatic systems such as human liver microsomes (HLM), differentiated HepaRG cells and human liver homogenate as well as in the presence of isolated enzymes (horse radish peroxidase, soybean lipoxygenase and human myeloperoxidase) and human promyelotic leukemia cells (HL 60), which contain human myeloperoxidase (Maseneni et al., 2012).

2. Material and Methods

2.1. Chemicals and Reagents

Metamizole, *N*-methyl-4-aminoantipyrine (4-MAA), 4-aminoantipyrine (4-AA), N-formyl-4-aminoantipyrine (4-FAA), *N*-acetyl-4-aminoantipyrine (4-AAA), ticlopidine, sulfaphenazole, (+)-N-3-benzylnirvanol, methylpyrazole, montelukast, PF-06281355, rifampicin and 3-methylcholanthrene were purchased from Sigma-Aldrich (Buchs, Switzerland). 4-MAA-d3.

4-AA-d3, 4-AAA-d3, bisoprolol-d5, 8′-hydroxyefavirenz, efavirenz-d4, flurbiprofen, 4′-hydroxyflurbiprofen, flurbiprofen-d4, omeprazole, 5′-hydroxyomeprazole, omeprazole-d3, metoprolol, α-hydroxymetoprolol, metoprolol-d7, tizanidine, hydroxytizanidine, tizanidine-d4, furaphylline, paclitaxel, 6α-hydroxypaclitaxel, chlorzoxazone, and 6-hydroxychlorzoxazone were acquired from TRC (Toronto, Canada). 1′-hydroxymidazolam and midazolam-d6 were obtained from Lipomed (Arlesheim, Switzerland). Midazolam and efavirenz were kindly provided by their manufacturers. Formic acid, HPLC grade methanol and HPLC grade water were purchased from Merck (Darmstadt, Germany). Cell culture media, fetal bovine serum, penicillin/streptomycin and Glutamax® were bought from GIBCO (Lucerne, Switzerland). Hydrocortison was obtained from Sigma-Aldrich (Buchs, Switzerland).

Stock solutions for the calibration curves were prepared in methanol (4-MAA, 4-AA, 4-FAA, 4-AAA, midazolam and 1′-hydroxymidazolam) or DMSO (tizanidine, hydroxytizanidine, efavirenz, 8′-hydroxyefavirenz, flurbiprofen, 4′-hydroxyflurbiprofen, omeprazole, 5′-hydroxyomeprazole, metoprolol, α-hydroxymetoprolol, paclitaxel, 6α-hydroxypaclitaxel, chlorzoxazone, and 6-hydroxychlorzoxazone). Stock solutions for the assays were prepared in water (4-MAA), methanol (midazolam) or DMSO (tizanidine, hydroxytizanidine, efavirenz, 8′-hydroxyefavirenz, flurbiprofen, 4′-hydroxyflurbiprofen, omeprazole, 5′-hydroxyomeprazole, metoprolol, α-hydroxymetoprolol, paclitaxel, 6α-hydroxypaclitaxel, chlorzoxazone, and 6-hydroxychlorzoxazone, rifampicin, 3-MC). The deuterated internal standards (IS) were prepared in methanol (4-MAA-d3: 150 ng/mL; 4-AA-d3: 20 ng/mL; 4-AAA-d3: 50 ng/mL; midazolam-d6: 100 ng/mL; metoprolol-d6: 12.5 ng/mL; bisoprolol-d5: 2.5 ng/mL; efavirenz-d5: 50 ng/mL; flurbiprofen-d3: 50 ng/mL; omeprazole-d3: 10 ng/mL; tizanidine-d4: 50 ng/mL; paclitaxel-d5: 200 ng/mL).

2.2. Microsomal Assay

Human liver microsomes (HLM; 0.5 mg microsomal protein), NADPH regenerating solutions A and B (*A*, contains $NADP^+$, glucose-6-phophate, and $MgCl_2$; *B*, contains glucose-6-phosphate dehydrogenase) were obtained from Corning Life science (Woburn, MA, USA). HLM were preincubated in potassium phosphate buffer (pH 7.4, final concentration 100 mM), and NADPH generating system for 5 min at 37 °C. The assay was started by the addition of 4-MAA (50 μM) or a control substrate (tizanidine (5 μM) for 1A2, efavirenz (10 μM) for 2B6, paclitaxel for (10 μM) for 2C8, flurbiprofen (5 μM) for 2C9, omeprazole (17 μM) for 2C19, metoprolol (20 μM) for 2D6, chlorzoxazone (1 μM) for 2E1, and midazolam (12 μM) for 3A4). The final volume of the assay was 1 mL. At time points 0, 1 h, 2 h, 4 h and 6 h, samples were taken and the reaction immediately stopped by adding 300 μL ice cold IS solution and subsequent vortex mixing.

In the case of inhibition assays, the HLM, the NAPDH regenerating system, and the respective CYP inhibitor were preincubated in potassium phosphate buffer (pH 7.4, final concentration 100 mM) for 5 min at 37 °C. Inhibitors were furaphylline for CYP1A2 (10 μM), ticlopidine for CYP2B6 (1 μM), montelukast for CYP2C8 (0.5 μM), sulfaphenazole for CYP2C9 (10 μM), (+)-N-3-benzylnirvanol for CYP2C19 (10 μM), quinidine for CYP2D6 (1 μM), methylpyrazole for CYP2E21 (1 μM), and ketoconazole for CYP3A4 (1 μM). For complete CYP inhibition, all inhibitors were combined. Assays were started by adding substrate solution and stopped as described above. All samples were stored at −20 °C until analysis.

2.3. Assays With HepaRG Cells

HepaRG cells were obtained from Biopredic International (Rennes, France) as undifferentiated cryopreserved cells. The cells were cultured in a 5% CO_2 and 95% humidified air environment at 37 °C. Freshly split cells were seeded in 96 well plates (10,000 cells/well) and treated for 4 weeks as previously described (Aninat et al., 2006). After differentiation, cells were induced with rifampicin (20 μM) or 3-methylcholanthrene (5 μM) for 3 days, while control cells were treated with vehicle (0.1% DMSO). Final vehicle concentration was 0.1%. Assays were started by replacing the induction medium with 50 μL fresh William's E medium containing 4-MAA or a control substrate (midazolam for rifampicin, tizanidine for 3-methylcholanthrene). During the assay, the plates were kept at 37 °C and 5% CO_2 in the cell culture incubator. The reaction was stopped by adding 150 μL of ice cold IS solution at selected time points (0, 15, 30, 45, 60, 75, 90, 105, 120 min). HepaRG cells were gently scratched from the bottom of the plate with a pipette tip and 150 μL were transferred into tubes. Samples were shaken for 1 min and stored at −20 °C until analysis.

2.4. Assays With Human Liver Homogenate

Part of a human liver biopsy (generously provided in anonymized form by Prof. Dr. med. L. Terracciano, Department of Pathology, University Hospital Basel) was cut into small cubes with a razor blade, weighed and transferred into a manual glass tissue grinder. Ice cold potassium phosphate buffer (100 mM, pH 7.4) containing NADPH (final concentration 1 mM) was added (3 times the weight of the liver cubes). The liver was homogenized on ice, transferred into Eppendorf tubes and put on ice. The substrates, 4-MAA (50 μM) and midazolam (12 μM), were dissolved in potassium phosphate buffer (100 mM, pH 7.4). The reaction was started by mixing 4 parts of liver homogenate (37 °C) and 1 part of the substrate solution (v/v), which was preheated to 37 °C (Graham, 2002). The final volume of the assay was 1 mL. Samples were withdrawn after 0, 15, 30, 45, 60, 75, 90, 105, 120 min and subsequently precipitated in 300 μL ice cold IS solution in order to terminate enzymatic reactions. Samples were shaken for 10 min and kept at −20 °C until analysis.

2.5. Assays With Horseradish Peroxidase and Soy Bean Lipoxygenase

4-MAA (50 μM) was preincubated in potassium phosphate buffer (50 mM, pH 7.4) containing hydrogen peroxide (final concentration 0, 10, 25, and 100 μM for assays with horse radish peroxidase, 1 mM for assays with soy bean lipoxygenase) for 5 min at 37 °C. Reactions were started by addition of purified enzyme (2 units/mL horse radish peroxidase, 10.8 μg/mL soy bean lipoxygenase). Samples were taken at 0, 5, 10, 15, 30, 60, 90 and 120 min and precipitated with ice cold methanol in a ratio of 1:3 (v/v). Samples were mixed for 1 min, diluted with IS solution (1:1 v/v), and then stored at −20 °C until analysis.

2.6. Assays With Human Myeloperoxidase

Human myeloperoxidase (MPO, Sigma-Aldrich, 0.5 units/mL) was dissolved in potassium phosphate buffer (50 mM, pH 7.4), 4-MAA was added (1, 2.5, 5, 10, 25, or 50 μM), and the mixture was preheated to 37 °C. Reactions were started by the addition of 100 μM hydrogen peroxide (100 μM final concentration). Samples (50 μL) were taken at 0, 2, 4, 8, 12, 16, 20 min. Enzyme kinetics were assessed within the first 4 min of the assay, because the 4-AA formation was linear in this time period. Reactions were terminated by the addition of ice cold methanol (150 μL). Samples were diluted (1:1 v/v) with IS solution, vortex mixed, and stored at −20 °C until analysis.

2.7. Assay With HL60 Cells

Human promyelocytic leukemia cells (HL60, CCL-240, lot number 7703261, ATCC, Wesel, Germany) were cultured in a 12 well plate (2,000,000 cells/well) using RPMI medium. Three different sets of the assay were applied. Set 1 consisted of viable HL60 cells, set 2 was carried out with viable HL60 cells but in the presence of a selective MPO inhibitor (PF-06281355, 30 µM), and set 3 was completed with heat inactivated HL60 cells (94 °C for 20 min). For each assay set, hydrogen peroxide was either added at time point zero, at the time points 0 and 60 min, or not at all. 4-MAA was added to the cells, which were kept at 37 °C, to start the assay. Samples were taken at 0, 5, 10, 15, 30, 60, 65, 70, 75, 90 and 120 min. Reactions were terminated by mixing the samples with ice cold methanol in a ratio of 1:3 (v/v) The samples were further 1:1 (v/v) diluted with IS solution and kept at −20 °C until analysis.

2.8. LC-MS/MS Analysis

Assay samples were thawed, vortex mixed, and centrifuged at 15 °C and 3220 g for 30 min. The analyte concentrations were determined by high performance liquid chromatography (HPLC, Shimadzu, Kyoto, Japan) tandem mass spectrometry (ABSciex, Ontario, Canada). An API 5500 Qtrap was used to analyze tizanidine, hydroxytizanidine, and tizanidine-d4. All other analytes were measured on an API 4000 mass spectrometer. All compounds were analyzed by electrospray ionization with multiple reaction monitoring (MRM) in positive polarity mode except chlorzoxazone, 6-hydroxychlorzoxazone, efavirenz, 8′-hydroxyefavirenz, efavirenz-d4, flurbiprofen, 4′-hydroxyflurbiprofen, and flurbiprofen-d3, which were negatively charged. Nitrogen was used in the ion source, and as curtain and collision gas. The LC-MS/MS systems were operated using Analyst software 1.6.2 (AB Sciex, Framingham, MA, USA).

Three LC methods (A, B, and C) were applied to analyze the compounds (summarized in Table 1). Water (mobile A) and methanol (mobile B), both supplemented with 0.1% formic acid, were used as mobile phases for the chromatography in method A and C whereas 0.01% acetic acid in water (mobile A) and methanol (mobile B) were used in method B.

Calibration lines were prepared in assay buffer and consisted of a blank sample and at least seven calibrators, which were injected twice, once at the beginning and once at the end of the run. Quality control samples (medium, high and low) were analyzed between the calibration lines along with the assay samples to ensure the integrity of the analysis. Sample concentrations were quantified by linear regression (weighting $1/x^2$) of the nominal analyte concentration (x) against the peak area ratio of the analyte and IS (y).

2.9. Statistics

Results are displayed as mean ± standard deviation of at least 3 independent experiments. Statistical analyses including Michaelis-Menten kinetics of the 4-AA formation were performed using GraphPad Prism 6 (GraphPad Software, La Jolla, CA, USA).

3. Results

3.1. 4-MAA Metabolism in Human Hepatic Systems

4-MAA was incubated in the presence of human liver homogenate (HLH), human liver microsomes (HLM), and HepaRG cells at a concentration of 50 µM and the formation of the metabolites 4-AA, 4-FAA and 4-AAA was monitored (Fig. 2). Metabolism of midazolam to 1-hydroxymidazolam was used to assure the functionality of the different hepatic systems.

The liver homogenate converted approximately 3% of the 4-MAA to 4-AA within 2 h of incubation (Fig. 2, 1a). The time to reach the maximal 4-AA concentration (1.5 µM) was 1.5 h. Midazolam was rapidly metabolized to 1-hydroxymidazolam; about 25% of MDZ was converted to 1-hydroxymidazolam and the maximal concentration of about 2.5 µM was reached after 30 min (Fig. 2, 1b). This proves the metabolic integrity of the liver homogenate.

Human liver microsomes converted approximately 1% of the 4-MAA to 4-AA and the metabolic process was not completed within the 6 h incubation time. A maximal 4-AA concentration of 0.5 µM was reached at the end of the experiment (Fig. 2, a). In comparison, 60% of the initial amount of midazolam was converted to 1-hydroxymidazolam and most of the metabolite was formed within the first 2 h of the incubation (Fig. 2, b).

HepaRG cells were differentiated to hepatocyte-like cells and their cytochrome content was induced with either rifampicin (CYP2B6, 2C9, 2C19, 3A4) or 3-MC (CYP 1A2) (Berger et al., 2016). The extent of induction was tested with midazolam and tizanidine, which are specific substrates for CYP 3A4 and 1A2, respectively. Rifampicin-induced HepaRG cells converted approximately 0.15% 4-MAA to 4-AA and the maximal 4-AA concentration (0.075 µM) was reached after 6 h, whereas non-induced cells were about 3 times less productive (Fig. 2, 3a). In contrast, 3-MC-treatment did not increase the 4-AA levels compared to non-treated cells (Fig. 2, 4a). Formation of 1-hydroxymidazolam and hydroxytizanidine was clearly induced by rifampicin and 3-MC treatment, respectively, demonstrating the suitability of the model. Formation of 4-FAA and 4-AAA was not detectable in any of the hepatic systems used (data not shown).

In the experimental systems used, 4-AA concentrations were highest in HLH followed by HLM and HepRG cells (Fig. 2). Since the microsomal protein content is about 40 mg protein per gram human liver (Zhang et al., 2015), the incubations with liver homogenate contained approximately 8 mg microsomal protein per assay (200 mg liver tissue per assay). In comparison, 0.5 mg microsomal protein was used per HLM assay. After 2 h of incubation, approximately 280 pmol and 1600 pmol 4-AA was formed in HLM and HLH, respectively (Fig. 2). Taking into account the microsomal protein content per assay, the 4-AA formation rate per mg microsomal protein per hour was about 280 pmol in HLM and 100 pmol in HLH. Hence, the microsomes were roughly three times more efficient in producing 4-AA than the HLH, suggesting that in the liver, the conversion of 4-MAA to 4-AA is performed within the microsomes.

3.2. Inhibition of 4-AA Formation in Human Liver Microsomes

CYP inhibition studies were carried out in HLM, because the conversion of 4-MAA to 4-AA could be determined with a robust assay and microsomes were more readily available than the other systems investigated. CYP inhibition studies were carried out in order to identify the responsible enzymes for 4-MAA demethylation. Hence, the metabolism of 4-MAA was studied with and without specific inhibitors of CYP1A2, 2B6, 2C8, 2C9, 2C19, 2D6, 2E1, and 3A4. Moreover, the inhibitory effect of all eight inhibitors combined was investigated. In parallel, the inhibitors were incubated also with the respective CYP-specific substrate in order to verify their inhibitory activity. All inhibitors visually decreased the metabolism of the specific CYP substrates (Fig. 3A). In comparison, formation of 4-AA appeared to be only slightly inhibited in the presence of inhibitors of CYP2B6, 2C8, 2C9, 2E1 and 3A4, but not by CYP1A2, 2C19 and 2D6. Accordingly, a mixture of all eight inhibitors resulted in a distinct inhibition of 4-MAA metabolism. The $AUC_{0\text{-}6h}$ was calculated with and without inhibitor. The inhibitors reduced the metabolism between 30% (1A2) and up to 90% (2D6) in the case of specific CYP substrates. The % inhibition of 4-MAA demethylation to 4-AA was around 15% for 2B6 and 3A4, about 20% for 2C9, 25% for 2C8 and 7% for 2E1 (Fig. 3B). All inhibitors together decreased the 4-MAA demethylation of by about 65%. These results show that the demethylation of 4-MAA to 4-AA is not specific for

Table 1
LC-MS methods used in this study.

LC method	Analyte	MRM (Q1 → Q3) [*m/z*]	Collision energy [V]	Polarity mode [+/−]	Calibration range [nM]
A	4-MAA	221.2 → 56.1	31	+	0.1–100 µM
	4-MAA-d3		46	+	–
	4-AA	204.2 → 56.2	71	+	0.01–10 µM
	4-AA-d3	207.2 → 56.2	46	+	–
	4-FAA	232.1 → 204.1	46	+	0.01–10 µM
	4-AAA	246.2 → 83.1	46	+	0.01–10 µM
	4-AAA-d3	249.2 → 84.1	61	+	–
	Midazolam	326.2 → 291.3	86	+	0.01–10 µM
	Midazolam-d6	331.6 → 296.0	41	+	–
	Hydroxymidazolam	342.2 → 324.0	61	+	0.01–10 µM
B	Efavirenz	313.8 → 246.6	−105	−	0.025–10 µM
	8′-hydroxyefavirenz	329.9 → 286.1, 257.8	−105	−	0.001–2.5 µM
	Efavirenz-d4	317.9 → 68.9	−70	−	–
	Flurbiprofen	243.0 → 199.0	−45	−	0.005–10 µM
	4′-hydroxyflurbiprofen	259.1 → 214.9	−50	−	0.005–10 µM
	Flurbiprofen-d3	246.0 → 202.0	−50	−	–
	Chlorzoxazone	167.709 → 131.8	−30	−	0.001–10 µM
	6-hydroxychlorzoxazone	183.782 → 119.8	−28	−	0.001–2.5 µM
	Omeprazole	346.2 → 198.2	46	+	0.001–5 µM
	5′-hydroxyomeprazole	362.2 → 214.1	41	+	0.001–10 µM
	Omeprazole-d3	349.2 → 198.1	41	+	–
	Metoprolol	268.2 → 116.2	11	+	0.0025–10 µM
	α-hydroxymetoprolol	284.2 → 116.2, 98.2	66	+	0.0025–2.5 µM
	Metoprolol-d7	275.307 → 123.3	31	+	–
	Paclitaxel	854.287 → 105.0, 569.2	107, 15	+	0.05–10 µM
	6α-hydroxypaclitaxel	870.203 → 104.9, 286.1	93, 23	+	0.05–10 µM
	Paclitaxel-d5	859.297 → 291.2, 569.2	27, 15	+	–
C	Tizanidine	255.14 → 44.1	81	+	0.01–10 µM
	Hydroxytizanidine	270.0 → 60.1	81	+	0.001–5 µM
	Tizanidine-d4	259.1 → 48.2	136	+	

LC method A: Analytical column: Atlantis® T3, 2.1 × 50 mm, 3 µm; Flow rate: 0.85 mL/min; Temperature: 45° C.
Gradient program: 0.5 min, 2% B; 0.51 min, 30% B; 2 min, 50% B; 2.5 min, 98% B; 3 min, 98% B; 3.01 min, 2% B; 3.5 min, 2% B.
LC method B: Analytical column: Atlantis® T3, 2.1 × 50 mm, 3 µm; Flow rate: 0.8 mL/min; Temperature: 45 °C.
Gradient program: 0–0.5 min, 0% B; 1.5 min, 95% B; 2.5 min, 95% B; 2.51 min, 0% B; 3 min, 0% B.
A tee union was used to inline dilute the sample with mobile phase A during the first 0.5 min of each run.
LC method C: Analytical column: Luna PFP column, 50 × 2 mm, 3 µm; Flow rate: 0.8 mL/min; Temperature: 45 °C.
Gradient program: 0–0.2 min, 5% B; 0.2 min, 50% B; 2 min, 95% B; 2.7 min, 95% B; 2.71 min, 5% B; 3 min, 5% B.

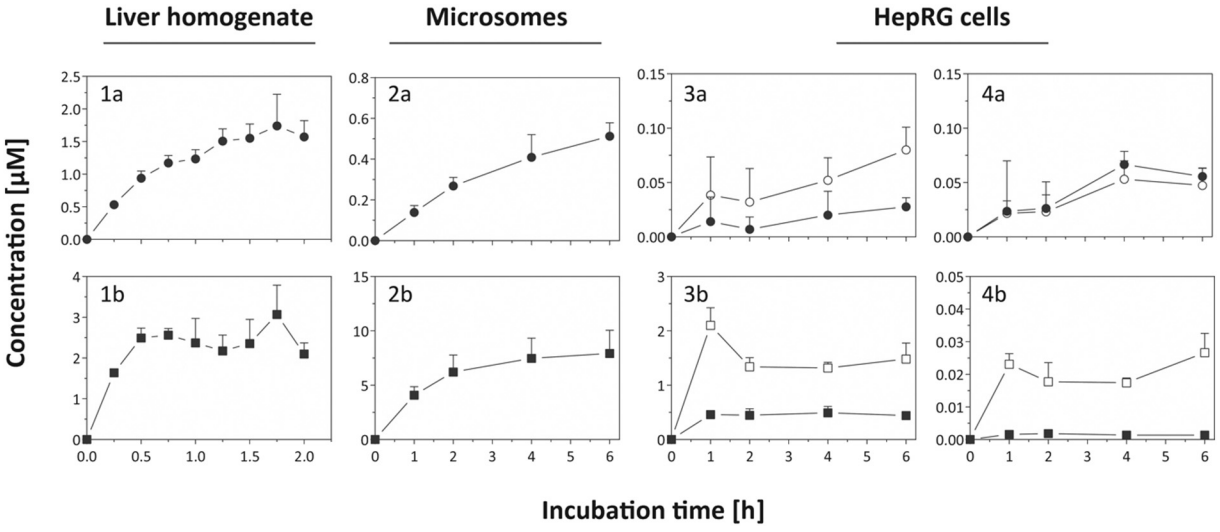

Fig. 2. *In vitro* metabolism of 4-MAA to 4-AA (-●-) mediated by different hepatic systems (upper row), namely liver homogenate (1), microsomes (2), and HepRG cells (3 and 4). HepRG were either not treated (-●-), or induced with rifampicin (-○-, 3) or 3-MC (-○-, 4). Metabolic activity of the hepatic systems was confirmed by the formation of hydroxy-midazolam (-■-, 1b-3b) and hydroxy-tizanidine (-■-, 4b) from midazolam or tizanidine, respectively (lower row). Hydroxy-midazolam (3b, -□-) and hydroxy-tizanidine (4b, -□-) formation was additionally monitored in rifampicin (3b) and 3-MC (4b) induced HepRG cells. Error bars correspond to the standard deviation (n = 3). Initial concentrations were 50 µM for 4-MAA, 12 µM for midazolam and 5 µM for tizanidine.

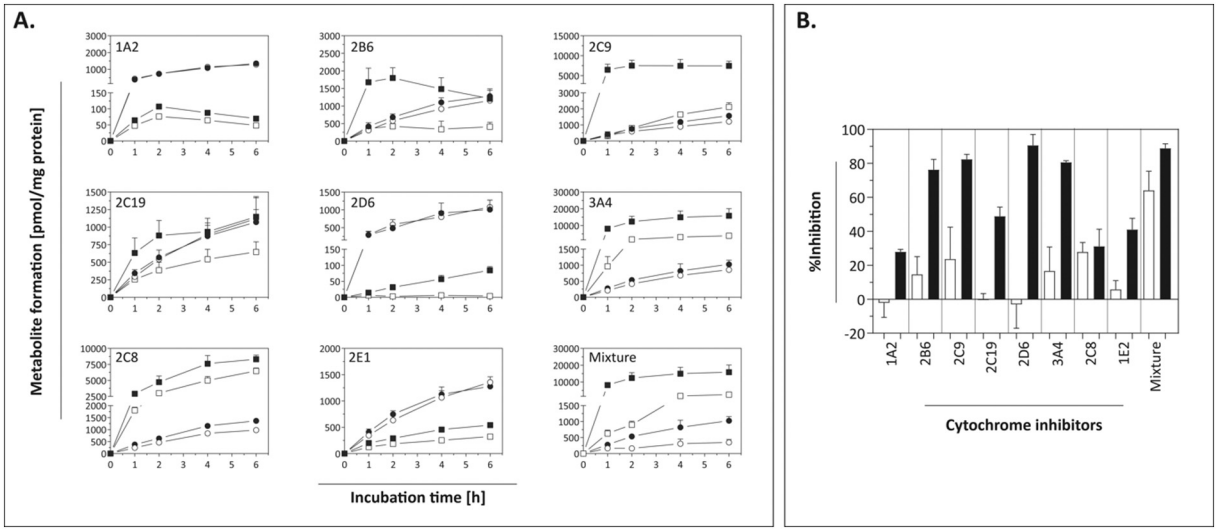

Fig. 3. A. Formation of 4-AA (-●-) and specific cytochrome substrates (-■-, 1A2: tizanidine, 2B6: efavirenz, 2C9:flurbiprofen, 2C19: omeprazole, 2D6: metoprolol, 3A4: midazolam, mixture: midazolam) in human liver microsomes. Specific cytochrome isoform inhibitors (1A2: furafylline, 2B6: ticlopidine, 2C8: montelukast, 2C9: sulfaphenazole, 2C19: (+)-N-3-benzylnirvanol, 2D6: quinidine, 2E1: methylpyrazole, 3A4: ketoconazole) and a mixture of all eight inhibitors were used to inhibit the formation of 4-AA (-○-) and of the known cytochrome substrates (-□-). B. Inhibition of 4-AA formation (white bars) and metabolite formation of specific cytochrome substrates (black bars). The % inhibition was calculated as $100 - \left(\frac{AUC_{with\ inhibitor}}{AUC_{without\ inhibitor}} \times 100\right)$. The area under the concentration-time curve (AUC) from time point zero to 6 h was determined using the linear trapezoidal rule. The error bars correspond to the standard deviation ($n = 3$).

one CYP.

3.3. 4-MAA Demethylation Catalyzed by Peroxidases

N-demethylation of xenobiotics can also be performed by other enzymes than cytochrome P450 oxidases, *e.g.* by peroxidases (Benedetti, 2001; Benedetti et al., 2009). We therefore incubated 4-MAA in the presence of HRP and different concentrations of hydrogen peroxide (0, 10, 25, and 100 µM), which acts as a cofactor of the enzyme. The decrease of 4-MAA depended visibly on the hydrogen peroxide concentration (Fig. 4A). 100 µM hydrogen peroxide led to complete degradation of 50 µM 4-MAA within 10 min, while 25, 10 and 0 µM produced a drop from 50 µM to 10, 30, and 45 µM, respectively. The 4-AA formation was also connected to the hydrogen peroxide concentration. Maximal 4-AA concentrations of about 1 µM, 6 µM and 10 µM were observed when 0, 10 or 25 µM hydrogen peroxide was added to the reaction mixture. Interestingly, 4-AA reached a maximal concentration of approximately 12 µM within 5 min of incubation when using 100 µM hydrogen peroxide and then decreased and had completely disappeared after 30 min. Hence, 4-AA is presumably an intermediate metabolite considering also that the mass balance between 4-MAA and 4-AA did not come out even. Importantly, hydrogen peroxide alone at a concentration of 100 µM formed only negligible amounts of 4-AA (~0.1 µM), showing that this reaction depends on the presence of HRP.

4-MAA was additionally incubated in the presence of soybean lipoxygenase and 100 µM hydrogen peroxide. In contrast to HRP, under these conditions, the 4-AA concentration increased steadily over 120 min and the 4-MAA concentration decreased in a similar manner as described above for HRP (data not shown).

Finally, the demethylation capability of a human peroxidase, namely myeloperoxidase, was tested for 4-MAA. Again, 100 µM hydrogen peroxide was used as a cofactor. Approximately 2% of 4-MAA was converted to 4-AA within 20 min of incubation, which did not lead to a measurable decrease of the 4-MAA concentration (50 µM). The increase of 4-AA was linear for the first 4 min but leveled off afterwards. Thus, Michaelis-Menten kinetics was determined based on the initial reaction rate (0–4 min), resulting in a K_m of 22.5 ± 3.7 µM and a V_{max} of 0.140 ± 0.009 nmol/min/0.5 U (equal to 10 µg protein) or 14 nmol/min/mg protein (Fig. 4B).

Overall, none of the investigated peroxidases was capable of producing 4-FAA or 4-AAA (data not shown).

3.4. 4-MAA Demethylation by HL-60 Cells

In a next step, we investigated whether 4-MAA demethylation is possible by HL-60 cells, which are known to express MPO (Maseneni et al., 2012). 4-MAA was incubated with viable HL60 cells, with viable HL60 cells plus a selective MPO inhibitor, and with heat inactivated HL60 cells (Fig. 5). For each setup hydrogen peroxide was either not added, or added once ($T = 0$ h) or twice (T = 0 h and 1 h). Without the addition of hydrogen peroxide, almost no 4-AA was formed, whereby viable cells produced more 4-AA than MPO-inhibited or heat inactivated cells. HL60 cells converted approximately 5% of 4-MAA to 4-AA when hydrogen peroxide was added at the beginning of the experiment. A second addition of hydrogen peroxide after 1 h incubation almost doubled the conversion of 4-MAA to 4-AA within 15 min. HL60 cells treated with a MPO inhibitor formed less than half of 4-AA compared with uninhibited cells (2% *vs.* 5%). Heat inactivation almost nullified the 4-AA formation so that 95% less 4-AA was produced compared to viable and untreated HL60 cells. 4-FAA and 4-AAA were not detected following incubation of 4-MAA in HL60 cells (data not shown).

4. Discussion

Metamizole is a commonly used analgesic drug; however, it has been withdrawn from market in several countries because of the risk of agranulocytosis (Hedenmalm and Spigset, 2002). Although the compound is marketed since almost 100 years, neither the mode of action, nor the mechanism of toxicity is entirely elucidated. Moreover, the enzymes involved in the metabolism of metamizole are mostly unknown. Considering this lack of knowledge, more data are needed to ensure a safe clinical use of metamizole. Here, we investigated the *N*-demethylation process of 4-MAA in different metabolic systems in order to increase our knowledge about metamizole metabolism.

First, 4-MAA demethylation was investigated in different hepatic models such as HLH, HLM, and HepaRG cells, since it has been

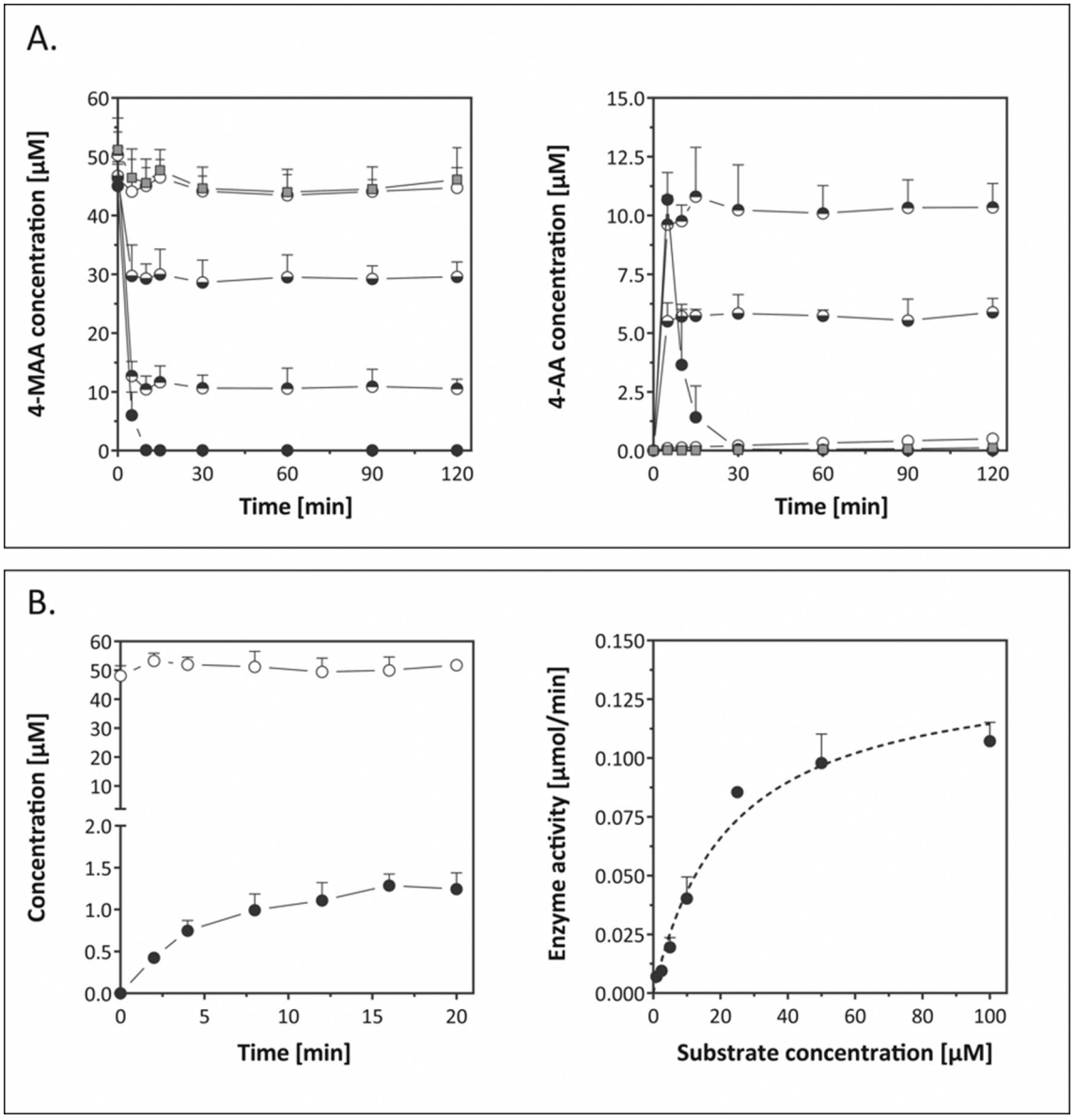

Fig. 4. A. Demethylation of 4-MAA (left graph) to 4-AA (right graph) catalyzed by horse radish peroxidase. Hydrogen peroxide at a concentration of 0 µM (-○-), 10 µM (-◒-), 25 µM (-◓-) and 100 µM (-●-) was used as co-factor. In addition, MAA was incubated with 100 µM hydrogen peroxide but without horse radish peroxidase (-■-). The error bars correspond to the standard deviation (n = 5). B. Demethylation of 4-MAA (-○-) to 4-AA (-●-) in the presence of human myeloperoxidase and 100 µM hydrogen peroxide (left graph, n = 5). Michaelis-Menten kinetics of the 4-AA formation catalyzed by human myeloperoxidase (right graph, n = 4). The error bars correspond to the standard deviation.

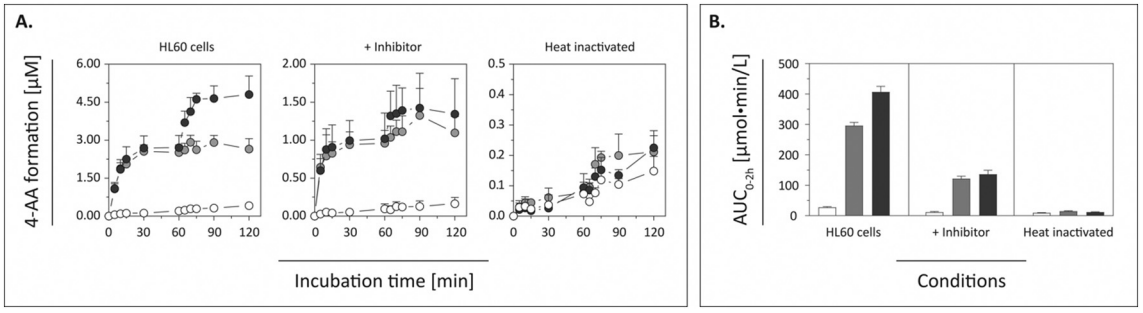

Fig. 5. A. Formation of 4-AA in the presence of HL60 cells. Hydrogen peroxide was either added at time point zero (-●-), or at the time points 0 and 60 min (-●-), or not at all (-○-). 4-AA formation in the presence of viable HL60 cells (left panel), of viable HL60 cells plus a selective MPO inhibitor (PF-06281355, 30 µM, middle panel), and of heat inactivated HL60 cells was investigated. B. AUC0-2 h determined for the different conditions. Coloring of the bars agrees with the concentration time profiles. The error bars correspond to the standard deviation.

demonstrated that 4-MAA can be demethylated by human liver microsomes (Geisslinger et al., 1996). All investigated hepatic models investigated were functional and able to form 4-AA. In relation to the estimated content of microsomes, HLM was more efficient in the demethylation of 4-MAA than HLH. In HLH, the metabolic activity may have been compromised by the thawing and homogenization process and/or the demethylation may have been impaired due to protein binding of 4-MAA (Zylber-Katz et al., 1985). In support of these assumptions, a reduced activity was not only present for 4-MAA demethylation but also for midazolam hydroxylation, which was about 30 times lower in HLH compared to HLM when calculated per mg microsomal protein. On the other hand, the data suggested that the hepatic demethylation of 4-MAA can largely be explained by microsomal metabolism.

Rifampicin, which induces CYP3A4, 2B6, 2C9 and 2C19 (Berger et al., 2016; Derungs et al., 2016), led to an approximately 4-fold higher 4-AA formation in treated compared to untreated HepaRG cells, which supports a CYP-dependent metabolism of 4-MAA (Berger et al., 2016). In contrast, up-regulation of CYP1A2 by 3-MC did not affect the 4-AA formation. CYP inhibition assays in HLM confirmed these results, since selective inhibition of CYP 1A2, 2C19, and 2D6 did not reduce 4-AA formation. In contrast, co-incubation with inhibitors for CYP3A4, 2B6, 2C8, 2C9 or 2E1 was associated with a small reduction of 4-AA formation. Inhibition of 4-MAA demethylation with the CYP3A4 inhibitor ketoconazole is in line with data described in literature (Geisslinger et al., 1996). Overall, inhibition of 4-MAA metabolism was generally low compared to the inhibition of the respective model compounds used; only a mixture of all eight CYP inhibitors was capable of inhibiting the demethylation rate by > 50%. Hence, the data indicate that hepatic 4-MAA demethylation is not performed by a specific CYP, but that several CYPs are contributing.

Based on the data of the current study, we can estimate the hepatic capacity for 4-MAA demethylation and compare it with the *in vivo* metabolism of 4-MAA. Using HLM, we observed a 4-MAA demethylation rate of 280 pmol/mg protein/h. A human liver weighs approximately 1500 g and 1 g liver contains approximately 40 mg microsomal protein (Zhang et al., 2015). Hence, assuming that 4-MAA is mainly metabolized in hepatic microsomes by CYPs, the *in vivo* capacity of 1 g liver is 40 × 280 pmol/h or 11.2 nmol/h and the hepatic capacity (1500 g) equals approximately 16.8 µmol/h. Following a single oral dose of 1 g metamizole (molecular weight: 311 g/mol) and assuming a bioavailability of 80%, approximately 2.6 mmol 4-MAA reaches the systemic circulation. The half-life of 4-MAA is about 2.7 h (Berger et al., 2016; Levy Micha, 1995), suggesting that at least 1.3 mmol 4-MAA can be eliminated during 2.7 h, corresponding to approximately 500 µmol/h. Since almost all 4-MAA is eliminated by demethylation, this number can be compared with the hepatic microsomal capacity of 16.8 µmol/h. This comparison suggests a large extrahepatic demethylation capacity for 4-MAA.

It has been shown that HRP is able to *N*-demethylate xenobiotic compounds and that soybean lipoxygenase is capable to demethylate aminopyrine, which differs only by a single methyl group from 4-MAA (Perez-Gilabert et al., 1997; Stiborova et al., 1997; Yang and Kulkarni, 1998). Hence, we incubated 4-MAA in the presence of HRP or soybean lipoxygenase, which both were capable to *N*-demethylate 4-MAA and to form 4-AA. Interestingly, in the presence of HRP, the 4-MAA concentration dropped to a higher extent than 4-AA was produced, suggesting the formation of metabolites other than 4-AA that we did not detect with our analytical method. It has been shown that, in the presence of HRP and hydrogen peroxide, the pyrazole ring of 4-MAA can be opened to form oxalic acid hydrazides, which could explain the mismatch of 4-MAA degradation and 4-AA formation (Wessel et al., 2006).

Based on these findings, we speculated that peroxidases could play a role in the metabolism of 4-MAA. Therefore, we tested human myeloperoxidase, which has a high activity in mature neutrophilic granulocytes and granulocyte precursors. 4-MAA demethylation by MPO could be described by Michaelis-Menten kinetics with a K_m of 22.5 µM and a maximal reaction velocity of 14 nmol/min/mg protein. The 4-MAA plasma concentrations following a single oral dose of 1 g reached serum concentrations in the range of the K_m (Levy Micha and Bernd, 1995), suggesting that MPO may play a role in the demethylation of 3-MAA *in vivo*. To further investigate this hypothesis, we roughly calculated the amount of MPO in human bone marrow in order to estimate the demethylation capacity by MPO. Assuming that the bone marrow corresponds to about 4% of the body weight and that about 50% of the bone marrow consists of hematopoietic cells, a person of 70 kg body weight has approximately 1.4 kg hematopoietic bone marrow. Of that, MPO expressing granulocytes and granulocyte precursors (promyelocytes, myelocytes, metamyelocytes and granulocytes) represent approximately 50% or 700 g (Donohue et al., 1958). Supposing an MPO protein content of 17 mg/g granulocytes (Schultz and Kaminker, 1962), the total amount in bone marrow would be about 12 g MPO protein. Taking into account the *in vitro* activity of 14 nmol/min/mg MPO protein, this results in a total activity of approximately 170 µmol/min or 10 mmol/h. Compared to the liver, the 4-MAA demethylation capacity of granulocytes and granulocyte precursors is approximately 600 times higher, underscoring the important role of extrahepatic demethylation of 4-MAA.

We also investigated 3-MAA demethylation in a more complex model than isolated MPO, namely in HL-60 cells, a granulocyte precursor cell line containing myeloperoxidase (Maseneni et al., 2012). Our experiments demonstrate that HL-60 cells are able to metabolize 4-MAA in the presence of hydrogen peroxide. The addition of a selective MPO inhibitor reduced 4-MAA demethylation by HL-60 cells significantly, proving the involvement of MPO in 4-MAA demethylation.

To the best of our knowledge, it has so far neither been shown that human MPO is capable of *N*-demethylation of small molecules, nor that it has a role in the metabolism of xenobiotics. Usually, plasma and blood concentrations of hydrogen peroxide are in the low µM range (Forman et al., 2016), but in granulocytes, hydrogen peroxide concentrations are higher and can rise up to 100 µM (Droge, 2002), suggesting that sufficiently high concentrations for 4-MAA demethylation can be reached.

Typically, peroxidase-derived oxidations are connected to radical formation (Campomanes et al., 2015; Hiner et al., 2002; Perez-Gilabert et al., 1997). It has for instance been shown that degradation of clozapine and amodiaquine by myeloperoxidase can lead to covalent binding of reactive metabolites to proteins in neutrophils, possibly explaining why these drugs are associated with agranulocytosis (Lobach and Uetrecht, 2014). Assuming that *N*-demethylation of 4-MAA may also take place in granulocyte precursors and granulocytes in the bone marrow, radical formation by this reaction could explain myelotoxicity of metamizole in susceptible persons. In support of this assumption, granulopoiesis has been described to be impaired on the promyelocyte stage in patients with metamizole-associated myoletoxicity (Kummer et al., 2006), the stage where myeloperoxidase has been shown to be present (Tsuruta et al., 1999).

In conclusion, the cytochrome P450 inhibition assays in HLM revealed that 4-MAA demethylation is not catalyzed by a specific CYP, but mainly by CYP3A4, 2B6, 2C8 and 2C9. Translation of our *in vitro* data into *in vivo* conditions suggest a dominant extra-hepatic metabolism of 4-MAA. In the presence of hydrogen peroxide, isolated human MPO was able to demethylate 4-MAA and the K_m of the reaction was in the same range as plasma concentrations of 4-MAA after therapeutic doses of metamizole. The demethylation capacity of granulocytes and granulocyte precursors was found to be considerably larger than the hepatic capacity and sufficiently large to account for the entire demethylation of 4-MAA to 4-AA in humans.

Conflict of interest

None of the authors has a conflict of interest regarding this study.

Financial support

The study was supported by a grant from the Swiss National Science foundation to SK (SNF 31003A_156270).

References

Agundez, J.A., Martinez, C., Benitez, J., 1995. Metabolism of aminopyrine and derivatives in man: *in vivo* study of monomorphic and polymorphic metabolic pathways. Xenobiotica 25, 417–427.
Alves, D., Duarte, I., 2002. Involvement of ATP-sensitive K(+) channels in the peripheral antinociceptive effect induced by dipyrone. Eur. J. Pharmacol. 444, 47–52.
Aninat, C., Piton, A., Glaise, D., Le Charpentier, T., Langouet, S., Morel, F., Guguen-Guillouzo, C., Guillouzo, A., 2006. Expression of cytochromes P450, conjugating enzymes and nuclear receptors in human hepatoma HepaRG cells. Drug Metab. Dispos. 34, 75–83.
Bast, A., Noordhoek, J., 1981. Product inhibition during the hepatic microsomal N-demethylation of aminopyrine in the rat. Biochem. Pharmacol. 30, 19–24.
Beirith, A., Santos, A.R., Rodrigues, A.L., Creczynski-Pasa, T.B., Calixto, J.B., 1998. Spinal and supraspinal antinociceptive action of dipyrone in formalin, capsaicin and glutamate tests. Study of the mechanism of action. Eur. J. Pharmacol. 345, 233–245.
Benedetti, M.S., 2001. Biotransformation of xenobiotics by amine oxidases. Fundam. Clin. Pharmacol. 15, 75–84.
Benedetti, M.S., Whomsley, R., Poggesi, I., Cawello, W., Mathy, F.X., Delporte, M.L., Papeleu, P., Watelet, J.B., 2009. Drug metabolism and pharmacokinetics. Drug Metab. Rev. 41, 344–390.
Berger, B., Donzelli, M., Maseneni, S., Boess, F., Roth, A., Krahenbuhl, S., Haschke, M., 2016. Comparison of liver cell models using the Basel phenotyping cocktail. Front. Pharmacol. 7, 443.
Campomanes, P., Rothlisberger, U., Alfonso-Prieto, M., Rovira, C., 2015. The molecular mechanism of the catalase-like activity in horseradish peroxidase. J. Am. Chem. Soc. 137, 11170–11178.
Derungs, A., Donzelli, M., Berger, B., Noppen, C., Krahenbuhl, S., Haschke, M., 2016. Effects of cytochrome P450 inhibition and induction on the phenotyping metrics of the Basel cocktail: a randomized crossover study. Clin. Pharmacokinet. 55, 79–91.
Donohue, D.M., Reiff, R.H., Hanson, M.L., Betson, Y., 1958. Quantitative measurement of the erythrocytic and granulocytic cells of the marrow and blood. J. Clin. Invest. 37, 1571–1576.
Droge, W., 2002. Free radicals in the physiological control of cell function. Physiol. Rev. 82, 47–95.
Duarte, I.D., dos Santos, I.R., Lorenzetti, B.B., Ferreira, S.H., 1992. Analgesia by direct antagonism of nociceptor sensitization involves the arginine-nitric oxide-cGMP pathway. Eur. J. Pharmacol. 217, 225–227.
Eagling, V.A., Tjia, J.F., Back, D.J., 1998. Differential selectivity of cytochrome P450 inhibitors against probe substrates in human and rat liver microsomes. Br. J. Clin. Pharmacol. 45, 107–114.
Ergün, H., Frattarelli, D.A.C., Aranda, J.V., 2004. Characterization of the role of physicochemical factors on the hydrolysis of dipyrone. J. Pharm. Biomed. Anal. 35, 479–487.
Escobar, W., Ramirez, K., Avila, C., Limongi, R., Vanegas, H., Vazquez, E., 2012. Metamizol, a non-opioid analgesic, acts via endocannabinoids in the PAG-RVM axis during inflammation in rats. Eur. J. Pain 16, 676–689.
Flusser, D., Zylber-Katz, E., Granit, L., Levy, M., 1988. Influence of food on the pharmacokinetics of dipyrone. Eur. J. Clin. Pharmacol. 34, 105–107.
Forman, H.J., Bernardo, A., Davies, K.J., 2016. What is the concentration of hydrogen peroxide in blood and plasma? Arch. Biochem. Biophys. 603, 48–53.
Geisslinger, G., Bocker, R., Levy, M., 1996. High-performance liquid chromatographic analysis of dipyrone metabolites to study their formation in human liver microsomes. Pharm. Res. 13, 1272–1275.
Graham, J.M., 2002. Homogenization of mammalian tissue. Sci. World J. 2, 1626–1629.
Gulmez, S.E., Gurdal, H., Tulunay, F.C., 2006. Airway smooth muscle relaxations induced by dipyrone. Pharmacology 78, 202–208.
Hedenmalm, K., Spigset, O., 2002. Agranulocytosis and other blood dyscrasias associated with dipyrone (metamizole). Eur. J. Clin. Pharmacol. 58, 265–274.
Hiner, A.N.P., Raven, E.L., Thorneley, R.N.F., Garcia-Canovas, F., Rodriguez-Lopez, J.N., 2002. Mechanisms of compound I formation in heme peroxidases. J. Inorg. Biochem. 91, 27–34.
Imaoka, S., Inoue, K., Funae, Y., 1988. Aminopyrine metabolism by multiple forms of cytochrome P-450 from rat liver microsomes: simultaneous quantitation of four aminopyrine metabolites by high-performance liquid chromatography. Arch. Biochem. Biophys. 265, 159–170.
Inoue, K., Fujimori, K., Mizokami, K., Sunouchi, M., Takanaka, A., Omori, Y., 1983. Simultaneous determination of aminopyrine hydroxylation and aminopyrine *N*-demethylation in liver microsomes by high-performance liquid chromatography. J. Chromatogr. 274, 201–208.
Kummer, O., Haschke, M., Tuchscherer, D., Lampert, M., Martius, F., Krahenbuhl, S., 2006. Agranulocytosis in a patient treated with metamizole and clopidogrel. In: Praxis (Bern 1994). 95. pp. 1743–1745 (quiz 1746-1747).
Levy Micha, Z.-K.E., Bernd, Rosenkranz, 1995. Clinical pharmacokinetics of dipyrone and its metabolites. Clin. Pharmacokinet. 28, 216–234.
Levy, M., Flusser, D., Zylber-Katz, E., Granit, L., 1984. Plasma kinetics of dipyrone metabolites in rapid and slow acetylators. Eur. J. Clin. Pharmacol. 27, 453–458.
Lobach, A.R., Uetrecht, J., 2014. Involvement of myeloperoxidase and NADPH oxidase in the covalent binding of amodiaquine and clozapine to neutrophils: implications for drug-induced agranulocytosis. Chem. Res. Toxicol. 27, 699–709.
Maione, S., Radanova, L., De Gregorio, D., Luongo, L., De Petrocellis, L., Di Marzo, V., Imming, P., 2015. Effects of metabolites of the analgesic agent dipyrone (metamizol) on rostral ventromedial medulla cell activity in mice. Eur. J. Pharmacol. 748, 115–122.
Maseneni, S., Donzelli, M., Taegtmeyer, A.B., Brecht, K., Krahenbuhl, S., 2012. Toxicity of clopidogrel and ticlopidine on human myeloid progenitor cells: importance of metabolites. Toxicology 299, 139–145.
Noda, A., Goromaru, T., Tsubone, N., Matsuyama, K., Iguchi, S., 1976a. *In vivo* formation of 4-formylaminoantipyrine as a new metabolite of aminopyrine. I. Chem. Pharm. Bull. (Tokyo) 24, 1502–1505.
Noda, A., Tsubone, N., Mihara, M., Goromaru, T., Iguchi, S., 1976b. Formation of 4-formylaminoantipyrine as a new metabolite of aminopyrine. II. Enzymatic demethylation and oxidation of aminopyrine and 4-monomethylaminoantipyrine. Chem. Pharm. Bull. (Tokyo) 24, 3229–3231.
Ortiz, M.I., Castaneda-Hernandez, G., Granados-Soto, V., 2003. Possible involvement of potassium channels in peripheral antinociception induced by metamizol: lack of participation of ATP-sensitive K+ channels. Pharmacol. Biochem. Behav. 74, 465–470.
Perez-Gilabert, M., Sanchez-Ferrer, A., Garcia-Carmona, F., 1997. Oxidation of aminopyrine by the hydroperoxidase activity of lipoxygenase: a new proposed mechanism of *N*-demethylation. Free Radic. Biol. Med. 23, 548–555.
Pierre, S.C., Schmidt, R., Brenneis, C., Michaelis, M., Geisslinger, G., Scholich, K., 2007. Inhibition of cyclooxygenases by dipyrone. Br. J. Pharmacol. 151, 494–503.
Schultz, J., Kaminker, K., 1962. Myeloperoxidase of the leucocyte of normal human blood. I. Content and localization. Arch. Biochem. Biophys. 96, 465–467.
Siebel, J.S., Beirith, A., Calixto, J.B., 2004. Evidence for the involvement of metabotropic glutamatergic, neurokinin 1 receptor pathways and protein kinase C in the antinociceptive effect of dipyrone in mice. Brain Res. 1003, 61–67.
Silva, L.C.R., Miranda e Castor, M.G., Souza, T.C., Duarte, I.D.G., Romero, T.R.L., 2015. NSAIDs induce peripheral antinociception by interaction with the adrenergic system. Life Sci. 130, 7–11.
Stiborova, M., Hansikova, H., Schmeiser, H.H., Frei, E., 1997. An investigation of the metabolism of *N*-nitrosodimethylamine and *N*-nitrosomethylaniline by horseradish peroxidase *in vitro*. Gen. Physiol. Biophys. 16, 285–297.
Tatsuo, M.A., Carvalho, W.M., Silva, C.V., Miranda, A.E., Ferreira, S.H., Francischi, J.N., 1994. Analgesic and anti-inflammatory effects of dipyrone in rat adjuvant arthritis model. Inflammation 18, 399–405.
Tortorici, V., Vasquez, E., Vanegas, H., 1996. Naloxone partial reversal of the antinociception produced by dipyrone microinjected into the periaqueductal gray of rats. Possible involvement of medullary off- and on-cells. Brain Res. 725, 106–110.
Tsuruta, T., Tani, K., Hoshika, A., Asano, S., 1999. Myeloperoxidase gene expression and regulation by myeloid cell growth factors in normal and leukemic cells. Leuk. Lymphoma 32, 257–267.
Valenzuela, F., García-Saisó, S., Lemini, C., Ramírez-Solares, R., Vidrio, H., Mendoza-Fernández, V., 2005. Metamizol acts as an ATP sensitive potassium channel opener to inhibit the contracting response induced by angiotensin II but not to norepinephrine in rat thoracic aorta smooth muscle. Vasc. Pharmacol. 43, 120–127.
Vanegas, H., Tortorici, V., Eblen-Zajjur, A., Vasquez, E., 1997. PAG-microinjected dipyrone (metamizol) inhibits responses of spinal dorsal horn neurons to natural noxious stimulation in rats. Brain Res. 759, 171–174.
Vasquez, E., Vanegas, H., 2000. The antinociceptive effect of PAG-microinjected dipyrone in rats is mediated by endogenous opioids of the rostral ventromedical medulla. Brain Res. 854, 249–252.
Volz, M., Kellner, H.M., 1980. Kinetics and metabolism of pyrazolones (propyphenazone, aminopyrine and dipyrone). Br. J. Clin. Pharmacol. 10 (Suppl. 2), 299S–308S.
Wessel, J.C., Matyja, M., Neugebauer, M., Kiefer, H., Daldrup, T., Tarbah, F.A., Weber, H., 2006. Characterization of oxalic acid derivatives as new metabolites of metamizol (dipyrone) in incubated hen's egg and human. Eur. J. Pharm. Sci. 28, 15–25.
Yang, X., Kulkarni, A.P., 1998. N-dealkylation of aminopyrine catalyzed by soybean lipoxygenase in the presence of hydrogen peroxide. J. Biochem. Mol. Toxicol. 12, 175–183.
Zhang, H., Gao, N., Tian, X., Liu, T., Fang, Y., Zhou, J., Wen, Q., Xu, B., Qi, B., Gao, J., Li, H., Jia, L., Qiao, H., 2015. Content and activity of human liver microsomal protein and prediction of individual hepatic clearance *in vivo*. Sci. Rep. 5, 17671.
Zylber-Katz, E., Granit, L., Levy, M., 1985. Plasma protein binding of dipyrone metabolites in man. Eur. J. Clin. Pharmacol. 29, 67–71.
Zylber-Katz, E., Granit, L., Levy, M., 1992. Formation and excretion of dipyrone metabolites in man. Eur. J. Clin. Pharmacol. 42, 187–191.